ELSEVIER

Comparative molecular modeling study of the three-dimensional structures of prostaglandin endoperoxide H2 synthase 1 and 2 (COX-1 and COX-2)

Marta Filizola,*† Juan J. Perez,* Albert Palomer,‡ and David Mauleón‡

**Department d'Enginyeria Quimica, Universitat Politecnica de Catalunya, ETS d'Enginyers Industrials, Barcelona, Spain*
†Centro di Ricerca Interdipartimentale di Scienze Computazionali e Biotecnologiche (CRISCEB), Seconda Universitá degli Studi di Napoli, Naples, Italy
‡Laboratorios Menarini, Badalona, Spain

*To understand the structural features that dictate the selectivity of diverse nonsteroidal antiinflammatory drugs for the two isoforms of the human prostaglandin H_2 synthase (PGHS), the three-dimensional (3D) structure of human COX-2 was assessed by means of sequence homology modeling. The ovine COX-1 structure, solved by X-ray diffraction methods and sharing a 61% sequence identity with human COX-2, was used as template. Both structures were energy minimized using the AMBER 4.0 force field with a dielectric constant of 4*r. *(*S*)*-Flurbiprofen, a nonselective COX inhibitor, and SC-558, a COX-2-selective ligand, were docked at the cyclooxygenase binding site in both isozymes, evidencing the role of different residues in the ligand–protein interaction. The 3D structures of the constructed four ligand–enzyme complexes were refined by energy minimization. Molecular dynamics simulations were also carried out, to understand more deeply the structural origins of the selectivity. Distances calculated during the dynamics process between the different ligands and the interacting residues of the two PGHS isozymes provided evidence of the flexible nature of the cyclooxygenase active site, permitting the identification of different conserved and nonconserved residues as responsible for ligand selectivity. © 1998 by Elsevier Science Inc.*

Address reprint requests to: Dr. Juan J. Perez, Department d'Enginyeria Quimica, Universitat Politecnica de Catalunya, ETS d'Enginyers Industrials, Av. Diagonal, 647, 08028 Barcelona, Spain.

Received 8 March 1997; revised 8 November 1997; accepted 2 December 1997.

Keywords: PGHS, COX, NSAIDs, AMBER force field, homology modeling

INTRODUCTION

Prostaglandin H_2 synthase (PGHS), also referred to as cyclooxygenase (COX), is a bifunctional enzyme that catalyzes the conversion of arachidonic acid into prostaglandin G_2 (PGG_2) and thence to prostaglandin H_2 (PGH_2) by means of its cyclooxygenase and peroxidase activity, respectively. PGH_2 is the precursor in the biosynthesis of a class of potent hormones including other prostaglandins, prostacyclins, and thromboxanes.[1,2] Cyclooxygenase activity of PGHS is competitively inhibited by a class of compounds known as nonsteroidal antiinflammatory drugs (NSAIDs). Members of this class include well-known therapeutic agents such as aspirin, ibuprofen, naproxen, and indomethacin.[3] Because some arachidonic acid metabolites processed by PGHS are known to be powerful mediators in the inflammatory response, NSAIDs achieve their analgesic, antiinflammatory, antipyretic, and antithrombogenic effects chiefly through blocking PGG_2 formation via the inhibition of PGHS. Noteworthy are the major side effects of NSAIDs, including their ulcerogenic and nephrotoxic activities.

There are at least two distinct PGHS isozymes, known as COX-1 and COX-2, whose expression is regulated differently. The former is constitutively expressed in most cells and tissues[4–6] and can respond instantaneously, producing prostaglandins that regulate events such as vascular homeostasis. Prostaglandin synthesis by this enzyme also helps to maintain normal stomach and renal functions. In contrast, COX-2 expression is induced in a number of cells by proinflammatory stimuli and

Journal of Molecular Graphics and Modelling 15, 290–300, 1997

655 Avenue of the Americas, New York, NY 10010

1093-3263/97/$17.00
PII S1093-3263(97)00107-1

by cytokines. Therefore, prostaglandins synthesized by this enzyme orchestrate prolonged physiological events such as inflammation, mitogenesis, and ovulation.[7,8] Hence, drug therapy aimed at reducing inflammation should be targeted toward isozyme 2. Most NSAIDs currently in clinical use have little selectivity and are known to inhibit both enzymes simultaneously, with the risk of causing ulcerogenic side effects during extended therapy periods most likely due to COX-1 inhibition in the gastrointestinal system. The identification and characterization of COX-2 have therefore led to the suggestion that the successful development of selective inhibitors may provide a new generation of NSAIDs with significantly reduced gastrointestinal toxicity.[9] At the present time some selective COX-2 inhibitors have already been disclosed, confirming the previous hypothesis.[4,9–12]

There must be differential structural features between the two isozymes responsible for the observed selectivity of some COX-2 inhibitors. The three-dimensional structure of ovine COX-1, complexed with the nonselective NSAID flurbiprofen, has been solved by X-ray diffraction methods.[13] The coordinates of the protein (but not those of the ligand), resolved to 3.5 Å are available as entry 1PRH from the Brookhaven databank. The same authors also solved the structure of the complex of the enzyme with different nonspecific ligands bound at the cyclooxygenase site, such as aspirin[14] or indomethacin.[15] These studies revealed that the cyclooxygenase-binding site is a long hydrophobic channel that extends from the membrane-binding domain to near the heme group. Residues at the cyclooxygenase-binding site identified to be directly involved in the ligand–enzyme interaction and later confirmed by site-directed mutagenesis studies[16] include Arg^{120}, Tyr^{355}, Tyr^{385}, and Ser^{530}. Moreover, involvement of residue Glu^{524}, forming a salt bridge with Arg^{120}, was also suggested.

Inspection of the nonconserved residues between COX-1 and COX-2 at the cyclooxygenase-binding pocket helped two research teams to suggest independently that residue Ile^{523} (a valine in COX-2) could be responsible for the observed ligand selectivity. Indeed, both laboratories convincingly demonstrated this hypothesis by site-directed mutagenesis experiments.[17,18] On the other hand, two crystal structures of the recombinant human[19] and mouse[20] COX-2 isozymes, complexed with different selective inhibitors, have been published. According to the authors, the structure of COX-2 exhibits the same geometric features as the ovine COX-1, a larger volume of the cyclooxygenase-binding pocket being one of the most significant differences exhibited by the former. Furthermore, crystal structures of COX-2 complexes provide evidence of the flexible nature of the cyclooxygenase active site of this isozyme. This was suggested on the basis of the conformational changes observed in the structure, owing to the interaction between residues Glu^{524} and Arg^{513} (histidine in COX-1) observed only with two selective COX-2 ligands.[19]

The present work was aimed at providing a more profound insight into the structural features governing the binding affinity and selectivity exhibited by different NSAIDs for the two isozymes. The first step was the construction of a three-dimensional model of the human COX-2, on the basis of the crystal structure of ovine COX-1 by homology modeling. In a second step, (*S*)-flurbiprofen (a nonselective COX inhibitor) and SC-588 (a COX-2-selective ligand) were docked into the cyclooxygenase-binding site of the two isozymes in order to identify residues responsible for their observed affinity and selectivity. Finally, 300-ps molecular dynamics simulations were carried out on each of the four complexes in order to investigate the dynamic behavior of ligand–receptor interactions.

METHODS

Sequence alignment of the PGHS isozymes

The sequence of the human COX-2 comprises 604 residues and was derived from the SwissProt database (entry PGH2-human). It shares high sequence homology (61% identity) with ovine COX-1 and it is consequently expected that the two enzymes exhibit a similar 3D structure. Figure 1 shows the sequence alignment of the two enzyme sequences. Numbering throughout this work refers to the ovine COX-1 sequence. Disregarding both protein termini, COX-2 presents only one insertion (Pro^{106}) compared with ovine COX-1; this is the largest sequence difference in the membrane-binding domain.

Construction of a COX-2 3D model

The crystal structure of both isozymes is homodimeric. However, because the cyclooxygenase-binding pocket is located far from the contact area between the two monomers, it is not necessary to consider the dimer in modeling enzyme–inhibitor complexes. The crystal structure of COX-1 comprises residues 33–586.[13] Regarding the missing residues, the first 24 correspond to the signal peptide that is cleaved after translocation of the protein, and segments 25–32 and 587–601 were disordered in the crystal structure and could not be resolved. On the other hand, in COX-2 there is an insertion of 18 residues at the C terminus. As in COX-1 both termini are very flexible and could not be resolved in the crystal structures reported.[19,20] However, neither of the termini is close to the cyclooxygenase-binding pocket and presumably they do not influence its structural features. Accordingly, homology modeling of COX-2 was carried out on the same portion of the protein as in the crystal structure of COX-1 reported.

AMBER 4.0[21] was used to construct a 3D structure of COX-2 according to the following procedure. Coordinates of the backbone atoms in COX-2 were set to the values of the corresponding atoms in COX-1. Similarly, coordinates of side-chain atoms of the conserved residues were set to the values of the corresponding coordinates of COX-1 atoms as well. In contrast, side chains of nonconserved residues were set in an extended conformation. The only insertion, Pro^{106}, is located on a loop that connects two helices of the membrane-binding domain. Coordinates of the atoms of this residue were inserted without perturbation of any secondary motif. AMBER 4.0 parameters of heme group complexed with a histidine residue were taken from the literature.[22,23] The resulting structure of COX-2 was energy minimized *in vacuo* using a dielectric constant of 4*r*, as previously recommended.[24] Minimization was carried out in two steps. First, only side chains and the coordinates of Pro^{106} were allowed to vary. In a second step the entire structure was completely relaxed. To carry out a proper comparison, the crystal structure of COX-1 was also energy minimized under the same conditions. The resulting structure exhibited a root mean square deviation (rmsd) of 1.6 Å from the starting X-ray structure when all the backbone atoms were compared, which represents a reasonable value considering the

Figure 1. Sequence alignment of the human prostaglandin endoperoxide H_2 synthase 2 (COX-2) with the ovine COX-1.

resolution of the crystal structure. On the other hand, after minimization, the constructed structure of COX-2 exhibited an rmsd of 1.3 Å with the minimized structure of COX-1, when all the backbone atoms are considered.[25]

Construction of the ligand–enzyme complexes

The structures of the ligands (*S*)-flurbiprofen and SC-558 were constructed using the PREP module of AMBER. Although flurbiprofen has a pK_a of about 4.5, the neutral species was considered in the present study in order to avoid any possibility that the electrostatic interactions of the carboxylate and the side chain of Arg^{120} could govern the docking of the ligand. It is not expected that this assumption would produce large errors in the modeling of the complex, because hydrogen bonds in salt bridges are somewhat longer than conventional hydrogen bonds, irrespective of whether the donor or the acceptor is charged.[26] Figure 2 shows the atom-numbering scheme used for the two molecules. Atomic partial charges for the molecules were generated by fitting the molecular electrostatic potential computed with an STO-3G basis set using the GAUSSIAN94 suite of programs.[27] Ligands were manually docked into the cyclooxygenase-binding pocket of COX-1 and COX-2, complying with the structural features of the interaction reported in the X-ray diffraction studies.[13,19,20] The initial position of each of the ligands in the two isozymes was identical. After ligands were properly oriented in both isozymes, systems were energy minimized using the AMBER 4.0 program[21] with a dielectric constant of 4*r*. This procedure was carried out in two different ways: (1) Complexes were constructed by docking the ligands into the crystal structure of COX-1 and into the unrefined model of COX-2 constructed by homology modeling, respectively, and subsequently energy minimized; (2) ligands were docked into the minimized structures of the two isozymes that had been previously obtained in the refinement process of the COX-2 model and the complexes were then energy minimized. In both cases, a conjugate gradient minimization was carried out until the rmsd of two successive iterations was less than 0.001 Å. The results of both minimizations yielded two structures with a very small rmsd in the backbone atoms, so we considered that the structures achieved the same local minimum by the two procedures. Display and examination of models were carried out using INSIGHTII (Molecular Simulations, San Diego, CA) on a Silicon Graphics Indigo 2 workstation.

Molecular dynamics simulations

Molecular dynamics (MD) simulations were performed at constant temperature with the system coupled to a thermal bath and using the AMBER 4.0 program.[21] MD trajectory calculations begun by heating the minimized structures up to 300 K over 100 ps at a constant rate of 30 K/10 ps. After the slow heating process, a 300-ps production run at a constant temperature of 300 K followed. The time step was set to 2 fs, using the SHAKE algorithm, and a cutoff of 11.5 Å was used to compute nonbonded interactions, that is, the nearest neighbor list was updated every 10 steps.

RESULTS AND DISCUSSION

Owing to the high degree of identity and functional similarity between ovine COX-1 and human COX-2, as expected the structure of COX-2 after energy minimization remained very similar to that of its template, with an rmsd computed over the backbone atomic coordinates of 1.3 Å.[25,28] The single amino acid insertion in COX-2 (Pro^{106}), located in a loop connecting two helices on the membrane-binding domain, did not perturb

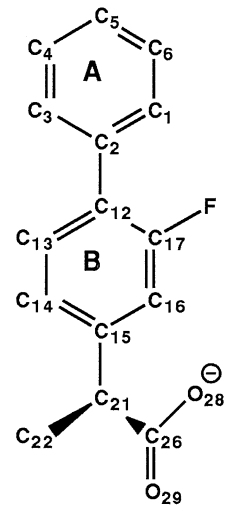

Flurbiprofen

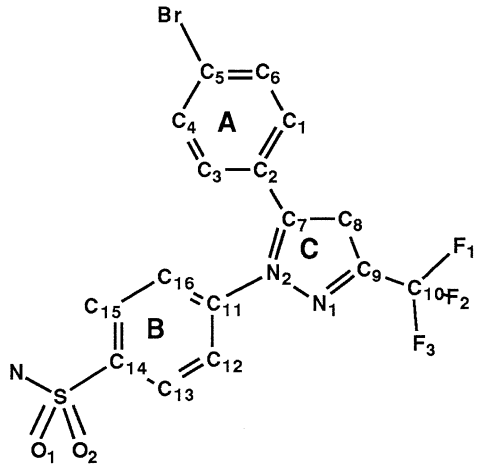

SC-558

*Figure 2. Atom-numbering scheme used for the nonselective NSAID (*S*)-flurbiprofen and the selective COX-2 ligand SC-558.*

the overall structure of the enzyme, in agreement with the reported crystal structures.[19,20] Superposition of the 3D structures of the two PGHS isoforms reveals only two nonconserved residues at the cyclooxygenase-binding site, Val^{523} and Arg^{513} (Ile^{523} and His^{513} in COX-1, respectively), which could be responsible for the selectivity exhibited by different ligands.

Docking of the nonselective COX inhibitor (*S*)-flurbiprofen and the selective COX-2 ligand SC-558 into the two isozymes was carried out in order to obtain a better understanding of ligand–receptor interactions. Thus, minimized structures of the four complexes were used to identify conserved and nonconserved residues in the neighborhood of the ligands. Figures 3 and 4 depict pictorially a comparison between the different residues involved in ligand–receptor interaction for the four complexes. Moreover, Table 1 lists values of the distances before and after minimization between selected residue side chains of the two isozymes and flurbiprofen, whereas Table 2 lists distances of the selected residue side chains of the two isozymes and SC-558.

Inspection of Tables 1 and 2 suggests that ligand selectivity is not only a consequence of the distinctive interactions with the two nonconserved residues at the cyclooxygenase-binding site, but also depends on the alternative interactions of the ligands with some of the conserved residues. Analysis of the interactions between flurbiprofen and the two isozymes permits the identification of nine residues (Tyr^{355}, Arg^{120}, Tyr^{385}, Ser^{530}, Leu^{352}, Trp^{387}, Tyr^{348}, Val^{349}, and Leu^{531}) that are in close proximity to the ligand. Distances summarized in Table 1 were computed from the center of the phenyl ring in Tyr^{385}, Trp^{387}, and Tyr^{348}; from atom C_ζ in Tyr^{355} and Arg^{120}; from

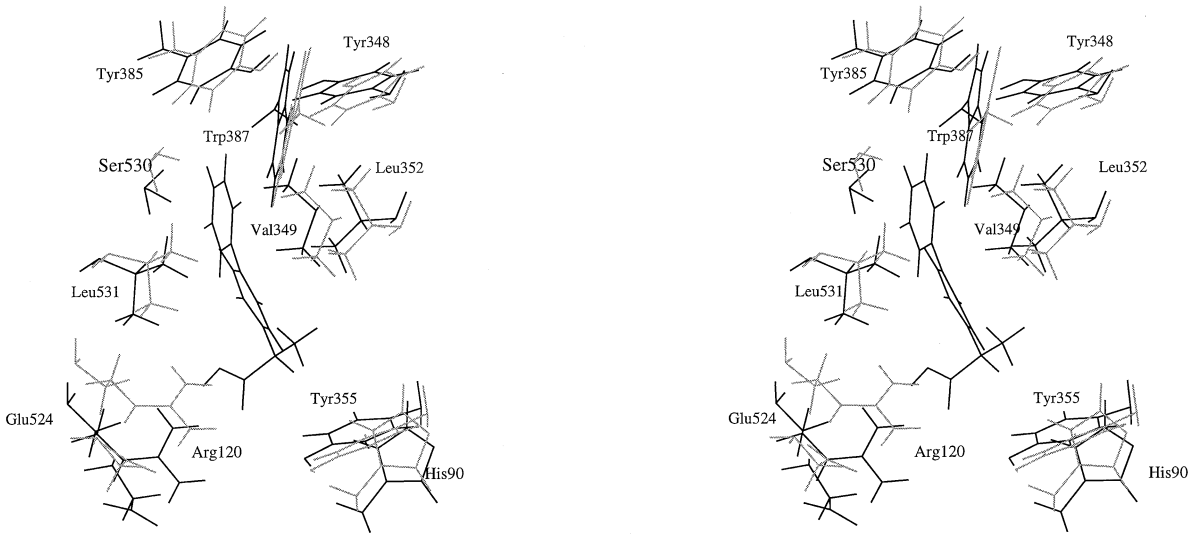

Figure 3. Illustration of the interacting residues of COX-1 (gray) and COX-2 (black) with flurbiprofen computed by superimposition of the complex energy-minimized structures.

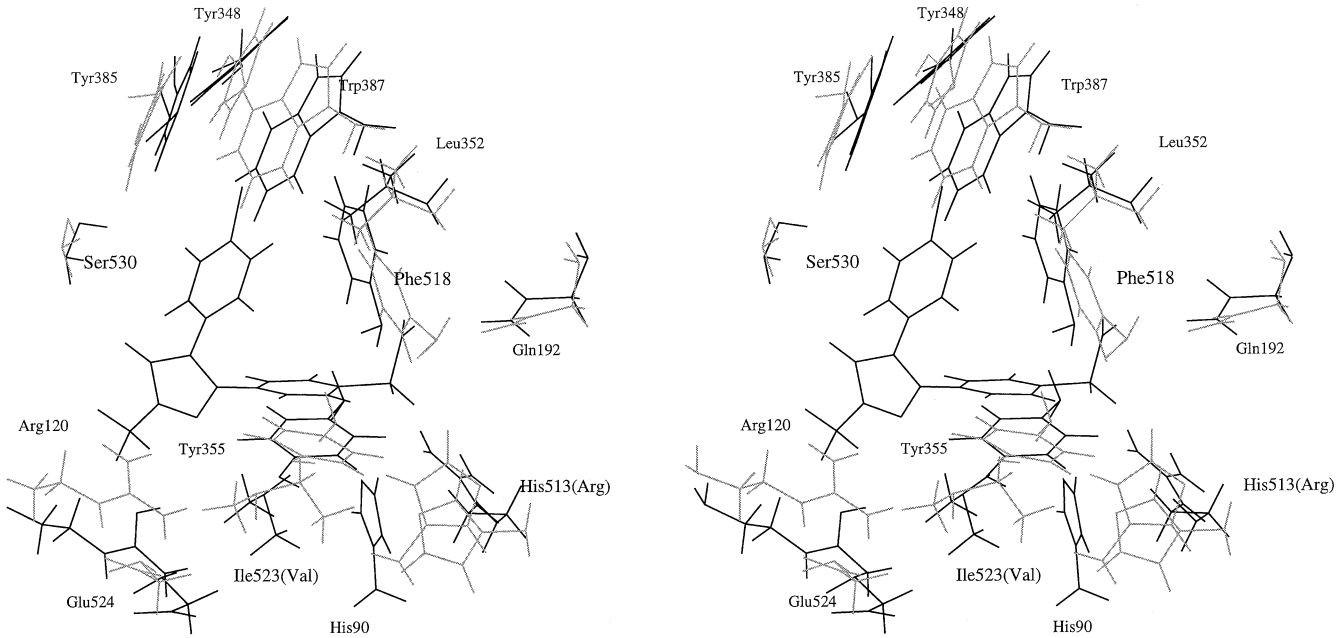

Figure 4. Illustration of the interacting residues of COX-1 (gray) and COX-2 (black) with SC-558 computed by superimposition of the complex energy-minimized structures.

atom C_γ in Leu^{352} and Leu^{531}; from atom C_β in Val^{349}; and from the hydroxyl hydrogen in Ser^{530}. Despite flurbiprofen being a nonselective ligand, it is a 10-fold better inhibitor of COX-1 (IC_{50} of 0.29 μM) than of COX-2 (IC_{50} of 2.56 μM).[29] This difference can be explained on the basis of a weaker interaction with the polar residues Tyr^{355} and Arg^{120} involved in the interaction with the carboxylate group of flurbiprofen, a consequence of the larger volume of the cyclooxygenase-binding pocket in COX-2; this makes it possible for the ligand to be less tightly bound. However, owing to the wide variety of mechanisms of inhibition of COX-1 and COX-2 (competitive, slow-onset, reversible, irreversible, partially irreversible, etc.), the difference can also be attributed to kinetics and need not necessarily be correlated with the binding affinities of the ligands.[19]

Table 2 lists distances between SC-558 and PGHS residues in close proximity to the ligand. Accordingly, 12 residues were identified as responsible for the ligand–receptor interaction: Tyr^{355}, Arg^{120}, Tyr^{385}, Ser^{530}, Ile^{523} (valine in COX-2), Phe^{518}, Leu^{352}, Trp^{387}, Tyr^{348}, Gln^{192}, His^{90}, and His^{513} (arginine in COX-2). Atoms involved in the computation of the intermolecular distances are those already mentioned in the case of the COX-1 complexes for the same residues, whereas C_β is considered for Ile^{523} (or Val^{523} of COX-2); the center of the side-chain ring for Phe^{518}, His^{90}, and His^{513}; and N_ϵ for Gln^{192}. SC-558 is a highly selective COX-2 inhibitor, with an IC_{50} of 0.0093 μM for COX-2 compared with an IC_{50} of 17.7 μM for COX-1.[29] Clearly, one of the reasons for its selectivity is the extra interaction with the nonconserved residue Arg^{513} (histidine in COX-1).[20] However, our modeling studies clearly point to additional structural features that induce SC-588 to bind to the two isozymes in a different manner, involving different residues and with the ligand bound in alternative orientations. Inspection of Table 2 shows that distances between the triflu-

Table 1. Values of distances between selected prostaglandin H_2 synthase side chains and the nonselective ligand (*S*)-flurbiprofen before and after minimization[a]

Flurbiprofen	COX-1	d_1 (Å)	d_2 (Å)	COX-2	d_1 (Å)	d_2 (Å)
C_{26}	Tyr^{355}	5.44	3.59	Tyr^{355}	4.11	4.22
	Arg^{120}	3.11	3.88	Arg^{120}	3.55	4.68
F	Ser^{530}	5.72	5.28	Ser^{530}	4.82	5.52
A (center)	Tyr^{385}	6.20	6.60	Tyr^{385}	5.99	6.10
	Trp^{387}	7.49	7.02	Trp^{387}	7.41	5.31
	Tyr^{348}	5.22	6.07	Tyr^{348}	5.65	7.61
	Leu^{531}	6.56	6.14	Leu^{531}	6.39	8.01
B (center)	Val^{349}	3.99	4.73	Val^{349}	3.92	5.22
	Leu^{352}	6.49	5.53	Leu^{352}	6.43	5.39

[a] d_1, distance before minimization; d_2, distance after minimization.

Table 2. Values of distances between selected prostaglandin H_2 synthase side chains and the COX-2-selective ligand SC-558 before and after minimization[a]

SC-558	COX-1	d_1 (Å)	d_2 (Å)	COX-2	d_1 (Å)	d_2 (Å)
C_{10}	Tyr^{355}	6.71	8.51	Tyr^{355}	7.67	5.87
	Arg^{120}	2.77	6.84	Arg^{120}	2.77	4.28
	Ser^{530}	7.60	2.42	Ser^{530}	7.60	7.74
B (center)	Ile^{523}	3.49	5.51	Val^{523}	3.52	4.03
	Phe^{518}	4.27	5.41	Phe^{518}	4.27	6.04
	Leu^{352}	3.32	5.14	Leu^{352}	3.32	6.47
A (center)	Tyr^{385}	7.51	6.15	Tyr^{385}	7.51	8.04
	Trp^{387}	5.45	4.60	Trp^{387}	5.45	7.53
	Tyr^{348}	7.31	5.55	Tyr^{348}	7.31	7.45
S	Gln^{192}	4.73	6.25	Gln^{192}	4.73	5.39
	His^{90}	5.56	3.05	His^{90}	5.56	5.74
	His^{513}	5.81	4.78	Arg^{513}	6.74	5.32

[a] d_1, distance before minimization; d_2, distance after minimization.

oromethyl group of SC-558 and the side chains of residues Tyr^{355} and Arg^{120} are longer in COX-1 than in COX-2, whereas the distance from the same group to the Ser^{530} side chain is much shorter. Clearly, in COX-2 the trifluoromethyl group interacts with residues Tyr^{355} and Arg^{120}, whereas in COX-1 this moiety interacts with the hydroxyl group of the Ser^{530} side chain, forcing the ligand to be docked in an alternative position, being pushed to the top of the binding pocket. This differential binding mode can be directly attributed to the steric hinderance caused by Ile^{523} (valine in COX-2).

Comparing the results of Tables 1 and 2, it clearly appears that docking of the nonselective inhibitor flurbiprofen is very similar for the two isozymes. In contrast, the presence of the nonconserved residues Ile^{523} (valine in COX-2) and His^{523} (arginine in COX-2) determines the different binding mode of SC-558 in the two cyclooxygenase-binding sites. A strong proton acceptor group, such as the carboxylate, originates an interaction with residues Tyr^{355} and Arg^{120} at the bottom of the cyclooxygenase-binding site, whereas the trifluoromethyl group, a weaker hydrogen bond acceptor, does not attract the ligand so tightly. This could be one of the features leading to selective inhibition, because replacement of the trifluoromethyl group in SC-558 results in compounds with poor selectivity.[20]

Analysis of the minimized structures of the complexes also reveals that residues Tyr^{355} and Arg^{120} are involved in intramolecular interactions with residues His^{90} and Glu^{524}, respectively. Table 3 shows the values of the intramolecular distances before and after the minimization of the PGHS complexes with flurbiprofen and SC-558. Specifically, distances are computed between the C_ζ atoms of Arg^{120} and Glu^{524} and between the C_ζ atom of Tyr^{355} and the side-chain ring center of His^{90}. The distance between the C_ζ atom of Glu^{524} and the side-chain ring center of His^{513} (or the C_ζ atom of arginine in COX-2) is also listed in Table 3. Residue Glu^{524} forms a salt bridge with Arg^{120} and its involvement in NSAID binding to the cyclooxygenase site had already been suggested by other researchers.[13] Furthermore, it has also been suggested[19] that Arg^{513} in COX-2 (histidine in COX-1) at the bottom of the cyclooxygenease-binding pocket could be involved in the formation of a salt bridge with Glu^{524} induced by COX-2-selective ligands. This hypothesis is not supported by this minimized model. In our calculations, distances computed between Arg^{120} and Glu^{524} in COX-1 and COX-2 (Table 3) clearly suggest a strong intramolecular interaction in the presence of both flurbiprofen and SC-558. In contrast, the distance between His^{513} in COX-1 or

Table 3. Values of selected intramolecular distances before and after minimization in the prostaglandin H_2 synthase complexes with (*S*)-flurbiprofen and SC-558[a]

Interacting COX-1 residues	d_1 (Å)	d_2 (Å)	Interacting COX-2 residues	d_1 (Å)	d_2 (Å)
Complexes with flurbiprofen					
Arg^{120}–Glu^{524}	4.80	3.98	Arg^{120}–Glu^{524}	4.80	3.78
Tyr^{355}–His^{90}	6.10	5.57	Tyr^{355}–His^{90}	6.10	5.16
His^{513}–Glu^{524}	7.91	11.41	Arg^{513}–Glu^{524}	9.31	11.68
Complexes with SC-558					
Arg^{120}–Glu^{524}	4.83	3.97	Arg^{120}–Glu^{524}	4.80	3.86
Tyr^{355}–His^{90}	6.10	5.47	Tyr^{355}–His^{90}	6.10	5.49
His^{513}–Glu^{524}	7.91	10.42	Arg^{513}–Glu^{524}	9.31	11.81

[a] d_1, distance before minimization; d_2, distance after minimization.

Arg^{513} in COX-2 and Glu^{524} appears very long in all the complexes.

To gain deeper insight into the important structural features that dictate ligand selectivity, we proceeded to monitor all of these distances along a molecular dynamics trajectory of 300 ps at a constant temperature of 300 K. Distances between Arg^{120} or His^{513} (arginine in COX-2) and Glu^{524} were computed every picosecond for the four complexes and are shown in Figure 5. Figure 5 shows that in the complexes of the two ligands with COX-1 (Figure 5A and B), the distance between residues

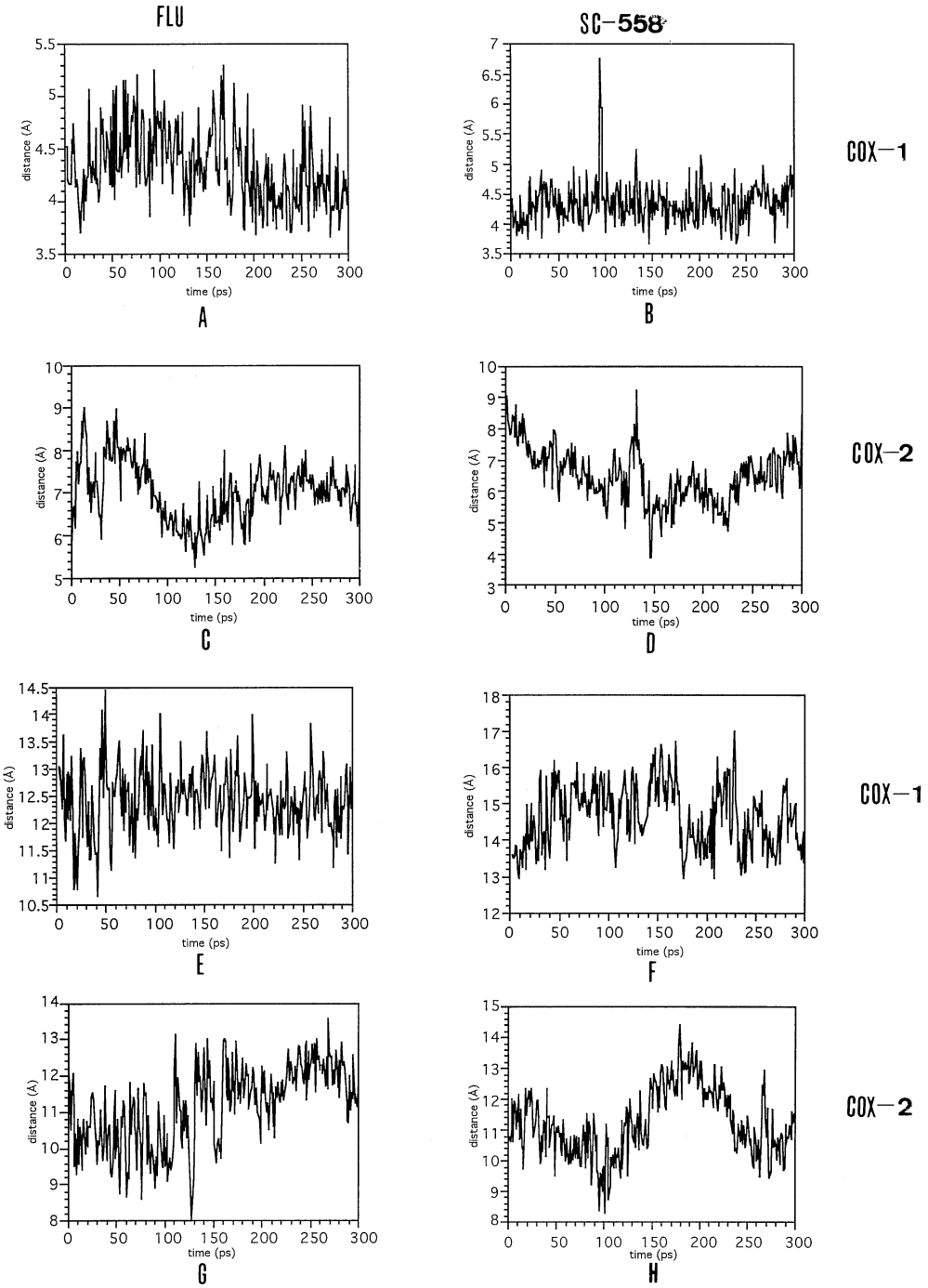

Figure 5. Distance variation between the residues Arg^{120} or His^{513} (arginine in COX-2) and Glu^{524} as determined in a dynamic process lasting 300 ps at a constant temperature of 300 K, carried out on the four PGHS models. (A) and (B) concern distance variation between Arg^{120} and Glu^{524} in the COX-1 complexes with flurbiprofen and SC-558, respectively, whereas (C) and (D) show those relative to COX-2; (E) and (F) illustrate the distance variation between His^{513} (arginine in COX-2) and Glu^{524} in the COX-1 complexes with flurbiprofen and SC-558, respectively, whereas (G) and (H) show those relative to COX-2.

Arg[120] and Glu[524] remains constant around a value of 4 Å. In contrast, the same distance in the COX-2 complexes (Figure 5C and D) exhibits larger fluctuations, with values around 7 Å. The distance between His[513] (arginine in COX-2) and Glu[524] was also monitored along the dynamic process. Figure 5E and F show that the interaction between the two residues is clearly nonexistent for the COX-1 complexes, with distance values around 12.5 and 15 Å, respectively. However, in the COX-2 complexes (Figure 5G and 5H), the distance between these two residues is shorter. Moreover, in the COX-2–SC-558 complex fluctuations exhibit periodic behavior (Figure 5H), supporting a fluctuating interaction between Arg[513] and Glu[524], in agreement with the existence of two alternative conformations of the receptor for ligand binding, as previously proposed.[19]

Figure 6 illustrates the fluctuation of the intramolecular distance between Tyr[355] and His[90], as determined in a molecular dynamic process, for the four systems studied. The two flurbiprofen complexes show similar behavior. In the complex with COX-1 (Figure 6A) there is a weak interaction between these two residues only during the first 50 ps. Subsequently the interaction is lost, although showing a tendency to recover at the end of the trajectory. In contrast, in the complex with COX-2 (Figure 6B), the interaction is maintained during the first 200 ps, and disappears in the last 100 ps. In the two SC-558 complexes the distance is shorter, with differential behavior in the two cases. Whereas in the COX-1 complex (Figure 6C) the interaction exhibits behavior similar to that observed in the fluorbiprofen complexes, in the COX-2 complex (Figure 6D) distance fluctuations are smaller, indicating that the interaction is kept during the whole trajectory. These results suggest that the proton-accepting strength of the group interacting with Arg[120] and Tyr[355] modulates the interaction between Tyr[355] and His[90]. Indeed, the carboxylate group of flurbiprofen avoids the interaction between the two residues, whereas the weaker proton-accepting trifluoromethyl group allows it. However, there is differential behavior between SC-558 docked in the two isozymes. This can be explained on the basis of the different orientation of the ligand when bound to the two isozymes. In COX-1 the interaction between Arg[120] and Tyr[355] is not disrupted by SC-558 because the ligand is far from these residues (see Table 2). However, in COX-2 the ligand is close enough to interact with Arg[120] but permits Tyr[355] not to be involved in this hydrogen-bonding network. These results advance our understanding of ligand selectivity.

Distances listed in Tables 1 and 2 were also monitored during the MD process, in order to understand the dynamic involvement of the different conserved and nonconserved residues in the interaction with the ligands during the dynamic process. The most illustrative graphs for flurbiprofen are shown in Figure 7, and those for SC-588 are shown in Figure 8. For the flurbiprofen complexes distances appear similar in both enzymes, although larger fluctuations are exhibited in the case of the COX-2 complex. The more significant differences are observed for the ligand and residues Tyr[355], Trp[387], Tyr[348],

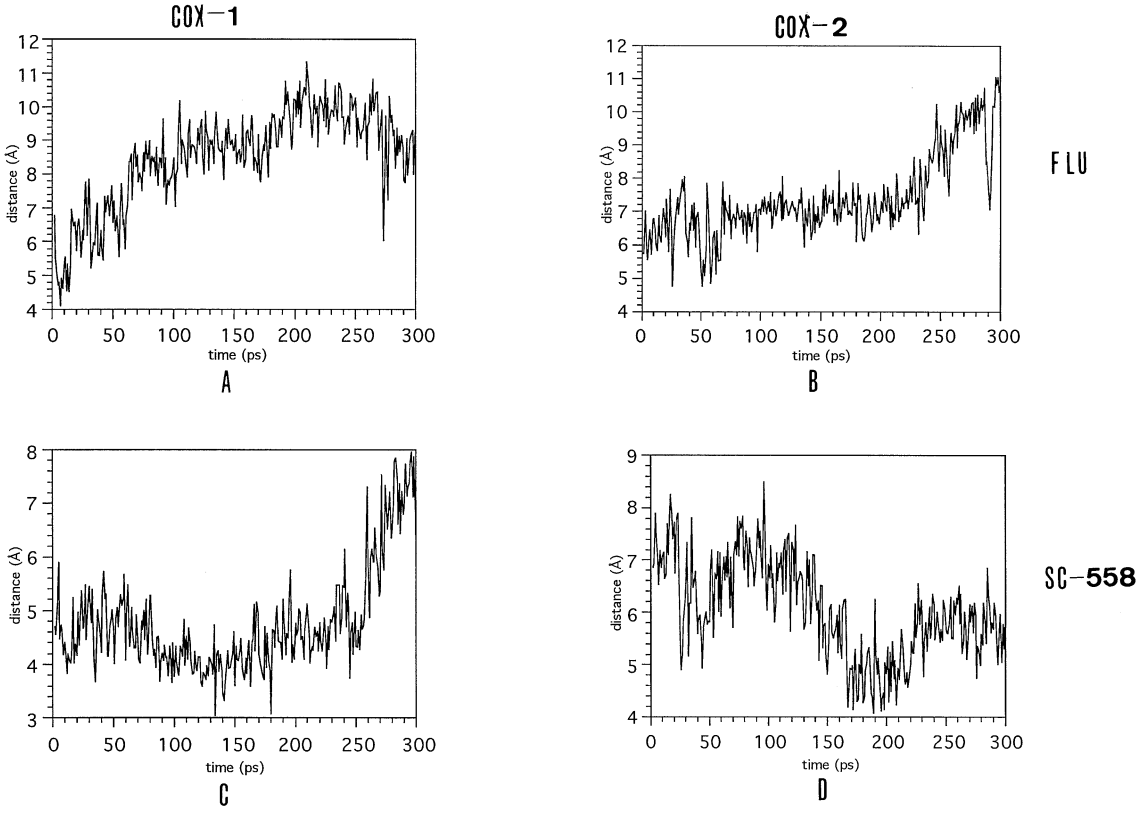

Figure 6. Variation of the intramolecular interaction between Tyr[355] and His[90] as determined in a dynamic process lasting 300 ps at a constant temperature of 300 K, and carried out on the four PGHS models. (A) and (B) concern COX-1 and COX-2 complexes with flurbiprofen, respectively; (C) and (D) illustrate the variation in the COX-1 and COX-2 complexes with SC-558, respectively.

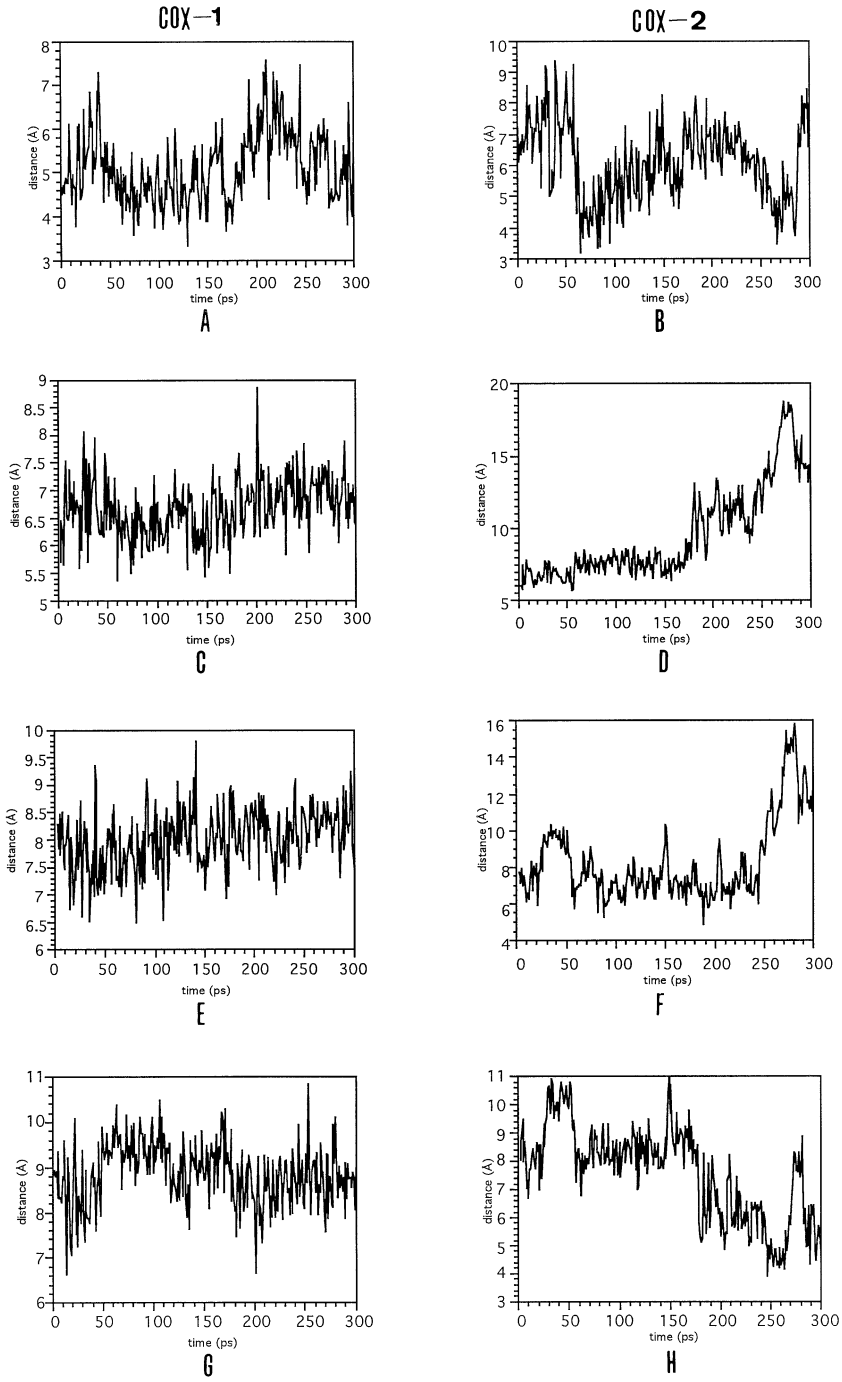

Figure 7. Graphics relative to the COX-1 and COX-2 complexes with flurbiprofen. (A) and (B) show the variation in the interaction of flurbiprofen with the Tyr[355] residue of COX-1 and COX-2, respectively. Distance variations between the Trp[387] and Tyr[348] residues and flurbiprofen are shown for the COX-1 complex in (C) and (E), respectively, whereas (D) and (F) concern the COX-2 complex. (G) and (H) show the distance variation from the ligand of Leu[531] in the COX-1 and COX-2 complexes, respectively.

and Leu[531]. The distance between flurbiprofen and Tyr[355] exhibits similar behavior in COX-1 and COX-2 (Figure 7A and B, respectively). With regard to residues Trp[387] and Tyr[348], distances in the COX-1 complex exhibit small fluctuations around the mean values (Figure 7C and E, respectively). In contrast, in the COX-2 complex (Figure 7D and F, respectively), these distances exhibit a tendency to increase at the end of the dynamic trajectory. Finally, in the case of Leu[531] the distance remains constant in the COX-1 complex (Figure 7*G*), whereas in the case of the COX-2 complex (Figure 7H) it decreases after the first 150 ps of the trajectory.

Figure 8 shows the most illustrative graphs regarding distances between selected residues of Table 2: Arg[120], Tyr[355], Tyr[385], Leu[352], Trp[387], and Arg[513] in both the PGHS complexes

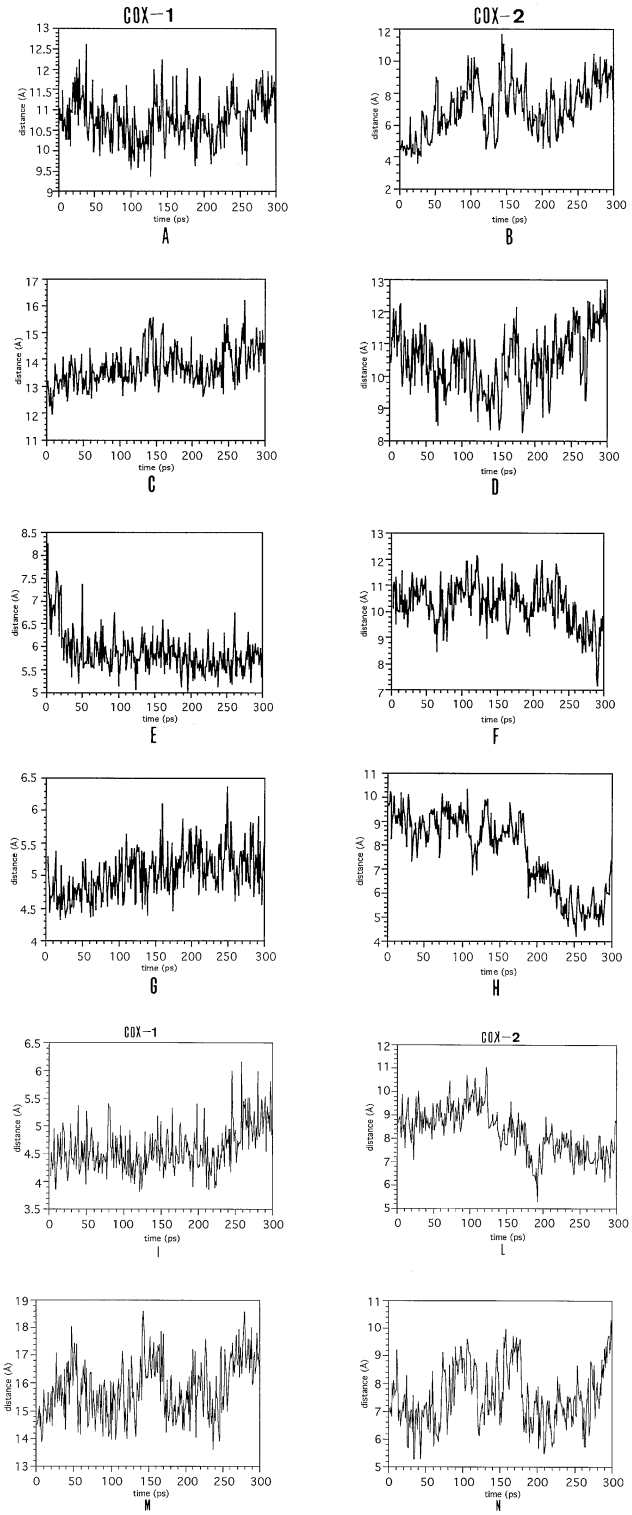

Figure 8. Results obtained for the residues Arg[120], Tyr[355], Tyr[385], Leu[352], Trp[387], and Arg[513] for both PGHS complexes with SC-558. (A), (C), (E), (G), (I), and (M) concern the intermolecular interactions between Arg[120], Tyr[355], Tyr[385], Leu[352], Trp[387], and Arg[513], respectively, in the COX-1 complex. (B), (D), (F), (H), (L), and (N) show the same interactions for the COX-2 complex with SC-558.

and SC-558 along the dynamics trajectory. In general terms, distances in the COX-2 complex exhibit larger fluctuations than in the COX-1 complex. The COX-1 distances with residues Arg[120] and Tyr[355] (Figure 8A and C) are long enough to consider the interaction as nonexistent. In the COX-2 complex (Figure 8B and D, respectively), the interactions exhibit large fluctuations, indicating the flexible nature of the cyclooxygenase-binding site, although interactions are generally maintained. Residue Tyr[385] keeps a strong interaction in the COX-1 (Figure 8E) complex, whereas this interaction is nonexistent in the COX-2 complex (Figure 8F). Interaction with Leu[352] is kept in both COX-1 (Figure 8G) as well in COX-2 complexes (Figure 8H), although distance fluctuations are different. Trp[387] exhibits a stronger interaction in COX-1 (Figure 8I) than in COX-2 (Figure 8L), although the interaction is maintained in the two cases along the entire production run process. Different behavior is exhibited by the distance between His[513] (arginine in COX-2) and the ligand in COX-1 and COX-2 (Figure 8M and N, respectively). It clearly appears that the interaction exists only for the COX-2 complex, in accordance with the previous experimental results.

CONCLUSIONS

The 3D structure of ovine COX-1 was used in the present work as a template with which to build a model of COX-2. Comparative analysis of the 3D structures of the two ligand–enzymes complexes reveals a difference of only two nonconserved residues at the cyclooxygenase-binding pocket, Ile[523] (valine in COX-2) and His[513] (arginine in COX-2), between the two enzymes at the cyclooxygenase-binding site. The nonselective inhibitor (*S*)-flurbiprofen and the COX-2-selective ligand SC-558 were docked into the cyclooxygenase-binding pocket in both structures. Residues of the two PGHS isozymes directly involved in the interaction with flurbiprofen and SC-558 were characterized both by energy minimization and molecular dynamics. The results of this work suggest that ligand selectivity cannot be explained only on the basis of the different interactions between the ligand and the nonconserved residues of COX-1 and COX-2, but is also due to alternative docking orientations of some ligands of different sizes and the consequent different interactions with several conserved residues of the binding pocket. Thus, selectivity of different ligands for the two COX isozymes is explained in addition to the role played by the nonconserved residues, in terms of the role played by the residues Glu[524], Arg[120], His[513] (arginine in COX-2), Tyr[355], and His[90] in intramolecular interactions.

REFERENCES

1 Garavito, R.M., Picot, D., and Loll, P.J. *Curr. Opin. Struct. Biol.* 1994, **4,** 529–535

2 Smith, W.L. and Marnett, L. J. In: *Metal Ions in Biological Systems* (Sigal, H. and Sigal, A., eds.). Marcel Dekker, New York, 1994, pp. 163–199

3 Loll, P. and Garavito, R.M. *Exp. Opin. Invest. Drugs* 1994, **3,** 1171–1180

4 Seibert, K., Zhang, Y., Leahy, K., Hauser, S., Masferrer, J., Perkins, W., Lee, L., and Isakson, P. *Proc. Natl. Acad. Sci. U.S.A.* 1994, **91,** 12013–12017

5 O'Neill, G.P. and Ford-Hutchinson, A.W. *FEBS Lett.* 1993, **330,** 156–160

6 Kargman, S., Chan, S., Evans, J., Vickers, P., and O'Neill, G.J. *Cell Biochem.* Suppl. **18B,** 1994, 319. [Abstract O109]
7 Hla, T., Ristimaki, A., Appleby, S., and Barriocanal, J.G. *Ann. N.Y. Acad. Sci.* 1993, **696,** 197–204
8 Herschman, H.R. *Cancer Metastasis Rev.* 1994, **13,** 241–256
9 Copeland, R.A., et al. *Proc. Natl. Acad. Sci. U.S.A.* 1994, **91,** 11202–11206
10 Futaki, F., Yoshikawa, K., Hamasaka, Y., Arai, I., Higuchi, S., Iizuka, H., and Otomo, S. *Gen. Pharm.* 1993, **24,** 105–110
11 Barnett, J., Chow, J., Ives, D., Chiou, M., Mackenzie, R., Osen, E., Nguyen, B., Tsing, S., Bach, C., Freire, J., Chan, H., Sigal, E., and Ramesha, C., *Biochim. Biophys. Acta* 1994, **1209,** 130–139
12 Ouellet, M. and Percival, M.D. *Biochem. J.* 1995, **306,** 247–251
13 Picot, D., Loll, P.J., and Garavito, R.M. *Nature (London)* 1994, **367,** 243–249
14 Loll, P.J., Picot, D., and Garavito, M. *Nature Struct. Biol.* 1995, **2,** 637–643
15 Loll, P.J., Picot, D., Ekabo, O., and Garavito, M. *Biochemistry* 1996, **35,** 7330–7340
16 Bhattacharya, D.K., Lecomte, M.C., Rieke, J., Garavito, R.M., and Smith, W.L. *J. Biol. Chem.* 1996, **271,** 2179–2184
17 Gierse, J.K., et al. *J. Biol. Chem.* 1996, **271,** 15810–15814
18 Guo, Q., Wang, L.-H., Ruan, K.-H., and Kulmacz, R.J. *J. Biol. Chem.* 1996, **271,** 19134–19139
19 Luong, C., Miller, A., Barnett, J., Chow, J., Ramesha, C., and Browner, M.F. *Nature Struct. Biol.* 1996, **3,** 927–933
20 Kurumbail, R.G., Stevens, A.M., Gierse, J.K., McDonald, J.J., Stegeman, R.A., Pak, J.Y., Gildehaus, D., Miyashiro, J.M., Penning, T.D., Seibert, K., Isakson, P.C., and Stallings, W.C. *Nature (London)* 1996, **384,** 644–648
21 Pearlman, D.A., Case, D.A., Caldwell, J.C., Seibel, G.L., Singh, U.C., Weiner, P., and Kollman, P.A. *AMBER 4.0.* University of California, San Francisco, 1991
22 Petrich, J., Lambry, J.-C., Kuczera, K., Karplus, M., Poyart, C., and Martin, J.-L. *Biochemistry* 1991, **30,** 3975–3987
23 Collins, J.R., Camper, D.L., and Loew, G.H. *J. Am. Chem. Soc.* 1991, **113,** 2736–2743
24 Harvey, S.C. *Proteins* 1989, **5,** 78–92
25 The rmsd between a structure of a protein built by homology modeling and its template varies with the degree of identity between the two sequences, ranging from 0.5 Å when identity is 85% to 1.7 Å when identity is 45% or even higher values for lower sequence identity
26 Jeffrey, G.A. and Saenger, W. In: *Hydrogen Bonding in Biological Molecules.* Springer-Verlag, Berlin, 1991, p. 371
27 Frisch, M.J., Trucks, G.W., Schlegel, H.B., Gill, P.M.W., Johnson, B.G., Robb, M.A., Cheeseman, J.R., Keith, T., Petersson, G.A., Montgomery, J.A., Raghavachari, K., Al-Laham, M.A., Zakrzewski, V.G., Ortiz, J.V., Foresman, J.B., Peng, C.Y., Ayala, P.Y., Chen, W., Wong, M.W., Andres, J.L., Replogle, E.S., Gomperts, R., Martin, R.L., Fox, J., Binkley, J.S., Defrees, D.J., Baker, J., Stewart, J.J.P., Head-Gordon, M., Gonzales, C., and Pople, J.A. *GAUSSIAN94,* revision B.2. Gaussian, Inc., Pittsburgh, Pennsylvania, 1995
28 Chothia, C. and Lesk, A.M. *EMBO J.* 1986, **5,** 823–826
29 Gierse, J.K., Hauser, S.D., Creely, D.P., Koboldt, C., Rangwala, S.H., Isakson, P.C., and Seibert, K. *Biochem. J.* 1995, **305,** 479–484